Supplementary Info: Multi-parameter photon-by-photon hidden Markov modeling

Paul David Harris*[1], Shimon Weiss[2,3], and Eitan Lerner†[1,4]

[1]Department of Biological Chemistry, The Alexander Silberman Institute of Life Sciences, Faculty of Mathematics & Science, The Edmond J. Safra Campus, The Hebrew University of Jerusalem, Jerusalem 9190401, Israel
[2]Department of Chemistry and Biochemistry, and Department of Physiology, University of California, Los Angeles, California, United States
[3]Department of Physiology, CaliforniaNanoSystems Institute, University of California, Los Angeles, California, United States
[4]The Center for Nanoscience and Nanotechnology, The Hebrew University of Jerusalem, Jerusalem 9190401, Israel

April 8, 2021

1 Data Analysis

1.1 H^2MM analysis

All code and raw data (in the form of photon-HDF5 files) is available for download here: (https://zenodo.org/record/4671393 [1]). Data must be extracted from the FRETbursts[2] data structure, and cast such that the H2MM_C package[3] can process it. In the H^2MM algorithm, photons are identified by an unsigned integer index, and an unsigned integer arrival time. A burst consists of two arrays of equal length, one for the indexes, and the other for the arrival times (in the form of one dimensional numpy arrays). The python function accepts as input an initiating H^2MM state model (implemented as a python extension type in the H2MM_C package[3]), a python list of the arrays of the photon indexes, and a separate python list of the arrays of the photon arrival times. FRETbursts identifies streams according to the following convention: the excitation period

*harripd@gmail.com
†eitan.lerner@mail.huji.ac.il

is identified as either Dex or Aex for donor or acceptor excitation respectively, and similarly, the detector at which the photon arrived is identified by either Dem or Aem for donor or acceptor emission respectively. Thus, for example a photon originating from donor excitation and arriving at the acceptor detector will be in the DexAem stream. In spH^{2}MM, only the DexDem and DexAem photon streams are used, with the DexDem photon stream assigned index 0, and the DexDem photon stream is assigned index 1. For mpH$_2$MM, the same convention is used, but the AexAem photon stream is also included, and assigned index 2. The AexDem photon stream should be exclusively background, and is therefore discarded for mpH^{2}MM analysis, however, it should be noted that the H2MM_C package is fully capable of incorporating the AexDem, or other photon streams, the exclusion is purely because the AexDem photon stream should not contain any useful information in two-color nanosecond alternating laser excitation (2c-nsALEX)[4] experiments (also known as pulsed-interleaved excitation, PIE[5]). Generally, any photon stream that contains useful information should be included in the analysis. Optimizations are run for a maximum of 7,200 iterations, or until the improvement in the loglikelihood between models was less than 10^{-14}, which is to a first approximation the precision available due to floating point errors. After model optimization, the *Viterbi* algorithm is used to both find the most likely state path through the data and within the given state model, and to calculate the ICL[6, 7]. For all data sets, H^{2}MM state models were optimized with increasing numbers of states, from one to four. If the four state model has the minimal ICL, then state models with larger number of states are optimized until the ICL ceases to improve. The function implementing the *Viterbi* algorithm in H2MM_C also sorts and characterizes the dwells automatically.

1.2 Parameter Calculations

The transition probability matrix contains the transitions rate constants in inverse units of the clock period of the measurement, that is the time period corresponding to one time interval of the measurement. For these measurements this is the pulsed laser repetition rate, which is 50 MHz in our experiments. Calculation of PR and S_{PR} is slightly more complicated, especially for mpH^{2}MM. Following the nomenclature of Lee *et. al.*[8], PR is generally defined as in Eq.S1:

$$PR = \frac{F_{D_{ex}}^{A_{em}}}{F_{D_{ex}}^{A_{em}} + F_{D_{ex}}^{D_{em}}} \tag{S1}$$

where $F_{D_{ex}}^{A_{em}}$ indicates the raw, uncorrected counts of acceptor photons during donor excitation period, (the counts in the DexAem photon stream) and $F_{D_{ex}}^{D_{em}}$ is likewise the raw, uncorrected donor counts during donor excitation period (the counts in the DexDem photon stream). S_{PR} is likewise defined in SP Eq.S2:

$$S_{PR} = \frac{F_{D_{ex}}^{A_{em}} + F_{D_{ex}}^{D_{em}}}{F_{D_{ex}}^{A_{em}} F_{D_{ex}}^{D_{em}} + F_{A_{ex}}^{A_{em}}} \tag{S2}$$

where, following the nomenclature $F_{A_{ex}}^{A_{em}}$ is the raw, uncorrected acceptor emission during acceptor excitation period (the counts in the AexAem photon stream). These values have clear equivalents in the emission probability matrix. From Pirchi *et. al.*[9] the emission probability matrix is defined as in Eq. S3:

$$(\hat{B}_{i,k}) \equiv b_{i,k} = P(y_t = k | x_t = i, \hat{\lambda}),\ for\ all\ t \\ and \begin{Bmatrix} 1 \leq i \leq N_s \\ 1 \leq k \leq N_p \end{Bmatrix} \quad \text{(S3)}$$

where $\hat{B}_{i,k}$ is the emission probability matrix, i is a given state, k is a given photon stream, y_t is the photon at time t, x_t is the state the system is in at time t, and $\hat{\lambda}$ is the H^{2}MM model. N_s and N_p are the maximum number of states and photon streams respectively.
It is also required that the emission probability matrix be row stochastic, as defined in Eq. S4:

$$\sum_{k=1}^{N-s} b_{i,k} = 1 \quad \text{(S4)}$$

Practically, we view the emission probability matrix as being the probability that a photon will belong to the stream k given the molecule is in state i. Therefore, we can make an equivalence between the F values from Lee *et. al.* and the elements of b as in Eq. S5:

$${}_iF_{k_{ex}}^{k_{em}} \equiv b_{i,k} \quad \text{(S5)}$$

Therefore, PR and S_{PR} of each state in a given H^{2}MM model are defined as in Eq. S6 and S7:

$${}^iPR = \frac{b_{i,DexAem}}{b_{i,DexAem} + b_{i,DexDem}} \quad \text{(S6)}$$

and

$${}^iS_{PR} = \frac{b_{i,DexAem} + b_{i,DexDem}}{b_{i,DexAem} + b_{i,DexDem} + b_{i,AexAem}} \quad \text{(S7)}$$

it should be noted that given the requirement of row stochasticity, the denominator of an spH^{2}MM model will be 1 in Eq. S6, and therefore the ${}^iPR_{spH^2MM} = b_{i,DexAem}$, but this does not hold true for mpH^{2}MM. Therefore practitioners of spH$_2$MM may be accustomed to simply looking at $b_{i,DexAem}$ as the ${}^iPR$, and must be careful to discontinue this practice when moving to mpH^{2}MM.

1.3 Viterbi Analysis

The H^{2}MM algorithm has no direct means to assess the error on individual values within a given state model for a given data set. However, the *Viterbi* algorithm provides a convenient way of obtaining a proxy for the error of individual values in a given H^{2}MM model. The process is the same as in Lerner *et. al.*[10]. After *Viterbi* analysis, consecutive photons classified as belonging to the same state are grouped into dwells.

1.3.1 *PR* and S_{PR} values

The counts of photons in each stream can then be used to assign each dwell a mean PR value, and for mpH^{2}MM, also a mean S_{PR} value. The definitions are essentially the same as those for bursts from Lee *et. al.*[8], and are given in Eq. S8 and S9:

$$PR_{dwell} = \frac{n_{dwell}^{DA}}{n_{dwell}^{DA} + n_{dwell}^{DD}} \tag{S8}$$

$$S_{PR,dwell} = \frac{n_{dwell}^{DA} + n_{dwell}^{DD}}{n_{dwell}^{DA} + n_{dwell}^{DD} + n_{dwell}^{AA}} = \frac{n_{dwell}^{DA} + n_{dwell}^{DD}}{n_{dwell}^{total}} \tag{S9}$$

where n_{dwell}^{stream} is the number of photons in originating from the given photon *stream*, with the first letter denoting the excitation period, and the second the detection channel. It should be noted that in spH^{2}MM $n_i^{DD} + n_i^{DA} = n_i^{total}$, and $S_{PR,dwell}$ cannot be calculated. It is then possible to define a ${}^{S}\bar{PR}_w$ and ${}^{S}\bar{S}_{PR,w}$ for each state S. As the total number of photons in each dwell varies, which could bias a traditional mean, we opt to use a weighted average instead, as defined in SI Eq S10 and S11:

$${}^{S}\bar{PR}_w = \frac{\sum_i^S (n_i^{DD} + n_i^{DA}) PR_i}{\sum_i^S n_i^{DD} + n_i^{DA}} \tag{S10}$$

$${}^{S}\bar{S}_w = \frac{\sum_i^S n_i^{total} S_i}{\sum_i^S n_i^{total}} \tag{S11}$$

where n_{dwell}^{total} is total number of photons in the dwell in all streams.
Their standard errors, as defined in SI Eq S12 and S13:

$$SE({}^{S}\bar{PR}_w) = \left[\frac{\sum_i^S (n_i^{DA} + n_i^{DD})(E_i - {}^{S}\bar{E}_w)^2}{\sum_i^S n_i^{DA} + n_i^{DD}} \right]^{1/2} / \sqrt{l_S} \tag{S12}$$

$$SE({}^{S}\bar{S}_{PR,w}) = \left[\frac{\sum_i^S n_i^{total} (S_i - {}^{S}\bar{S}_w)^2}{\sum_i^S n_i^{total}} \right]^{1/2} / \sqrt{l_S} \tag{S13}$$

where l_S is the number of dwells in state S.

1.3.2 Dwell time analysis

The difference in photon arrival times between the first photon in the dwell and the photon after the final photon in a dwell is characterized as the dwell duration, unless the dwell is the final dwell in the burst, in which case the difference is between the first and final photon in the dwell. A mean dwell time of dwells beginning in state g and transitioning to state h is then defined as in Eq. S14:

$$\bar{t}_{g,h} = \sum_{i=1}^{l_{g,h}} t_{i,g,h}/l_{g,h} \tag{S14}$$

The transition rate is $k_{g,h} = 1/\bar{t}_{g,h}$. The standard error of $t_{g,h}$ is defined as in Eq. S15:

$$SE(\bar{t}_{g,h}) = \left[\sum_{i=1}^{l_{g,h}} (t_{i,g,h} - \bar{t_{dwell,g,h}})^2/l_{g,h}\right]^{1/2} /\sqrt{l_{g,h}} \tag{S15}$$

Where $l_{g,h}$ is the number of dwells that start in state g and transition to state h. With the standard error of the transition rate begin defined as in Eq. S16:

$$SE(k_{g,h} = \frac{SE(\bar{t}_{g,h})}{\bar{t_{g,h}}} \tag{S16}$$

Occasionally the *Viterbi* algorithm predicts dwells with a very small number of photons, as these are likely spurious, we first exclude dwells from the analysis with 5 or fewer photons. Dwells at the beginning and end of bursts are truncated, and therefore we generally exclude them from the analysis to prevent them from biasing the results. However, when the transition rates approach the time scales of the burst (in the millisecond range), few dwells have a mean residence time in the burst, making the analysis often misleading. Therefore, we choose to analyse as separate data sets the durations of the dwells at the beginnings and ends of bursts. Differences in these three data sets and comparison with the mean dwell time must all be taken into consideration in assessing the validity of the extracted transition rates. On the whole however, we find that the transition probability matrix usually provides more reliable values than *Viterbi* derived mean dwell times. We also use the *Viterbi* results to flag transition rates as potentially spurious that have fewer than 10 detected dwells that have more than 5 photons in them.

1.3.3 Nanotime Analysis

As the arrival time relative to the last laser pulse (the nanotime) is also recorded, the fluorescent lifetime of bursts and sub-populations can be assesed. Using the *Viterbi* algorithm, each photon is assigned a sub-population. A histogram is then made of the nanotimes of all photons assigned to the same sub-population and stream, resulting in separate lifetime histograms for each photon stream in each sub-population. Since the *Viterbi* algorithm also includes a posterior

probability for each photon, giving in essence a likelihood that the assignment is correct, we implement a threshold, removing photons with a posterior probability of less than 0.2 from consideration. We find that increasing or decreaseing the threshold does not have a significant impact on the shape of the histograms, and thus the threshold is somewhat arbitrarily set, as a tradeoff between number of photons in the histogram reducing noise, and confidence of each photon assignment.

2 Microsecond ALEX Cautions

Periodic patterns brought on by the experimental setup, or other scientifically irrelevant factors may be detected by H^2MM. Therefore, microsecond ALEX (µsALEX)[8] is not well-suited to mpH^2MM. If the alternation period is slow, such that several photons are likely to arrive during one alternation of the laser excitation, this will create a periodic pattern in the data, which mpH^2MM will detect, creating states of entirely donor excitation, and entirely acceptor excitation, with transition rates equal to the alternation rate. Therefore no information about the actual S_{PR} values will be recoverable.

3 Model Selection

mpH^2MM is capable of detecting multiple parameters, however, it should not be assumed that a given sub-population is without its own hidden dynamics. Just as spH^2MM has difficulty distinguishing the open hairpin FRET sub-population and dark-acceptor sub-population, it is easy to imagine a similar situation occurring with mpH_2MM, the extra parameters only reduce the uncertainty and difficulty, they do not eliminate it. It is notable, however, that while the minimal ICL was found for the two-state model in spH^2MM, based on the less reliable BIC'[10], the three-state model would have been chosen. When comparing these models with the four-state mpH_2MM model, it is apparent that the three-state spH^2MM model exaggerates the difference between the dark-acceptor sub-population and the open hairpin FRET sub-population, but it is not entirely unreasonable (table S1. Over-fit models, based on the ICL therefore may suggest potential hidden sub-populations, but the parameter values of those sub-populations may not be reliable, due to lack of adequate information, either in number of photons or parameters. Therefore, all interpretations of any H^2MM results should rely not solely on the ICL or BIC' selection, but must take into account all prior knowledge, and perhaps invoke comparisons between apparently over- or under-fit models to best understand the data. The *Viterbi* algorithm, when used carefully, can also be useful in these circumstances. It must be understood that it finds the most probable state path, and that the photon streams are the result of several stochastic processes: fluorophore excitation, FRET and photon absorbtion by the detectors to name the primary ones. Therefore, it can never with absolute certainty, assign from which sub-

population a given photon originated. However, patterns are still often reflective of the true sub-population distribution. If the *Viterbi* is close to the truth, certain patterns should be present. First and foremost, the *Viterbi* derived ${}^{S}\bar{PR}_{w}$ and the ${}^{S}PR_{w}$ from the emission probability matrix should be similar, and the same for ${}^{S}\bar{S}_{PR,w}$ and ${}^{S}S_{PR,w}$ values. Additionally, the dwell-based $PR_{dwell,k}$ and $S_{PR,dwell,k}$ values should be centrally distributed around their mean values. These comparisons should all be taken into account when assessing the quality of a model.

4 Transforming a non-binomially distributed variables for work with mpH^{2}MM

Consider the variable t, which is best described as distributing as $\mathbf{P}(t)$. We want to map it to a parameter t' distributed by the beta distribution $\mathbf{B}(t')$. Since both are PDF's, their mapping should be performed on a basis of equal probabilities, which can be assesed according to their corresponding CDF's:

$$p = \int_{t_{min}}^{t} \mathbf{P}(t)\, dt = \int_{t_{min}}^{t} \beta(t')\, dt \tag{S17}$$

Eq. S17 will be the basis for transformation of a given t value to a given t' value. After this transformation, each t value can be transformed into a t' value for use as a parameter in the framework of mpH^{2}MM.
Let's take for example the donor photon nanotimes of in TCSPC-type smFRET measurements. We can accumulate all donor photon nanotimes into fluorescence decay. Fit with a sum of a few exponentials, and then define $\mathbf{P}(t)$. We would then need to define the exact α and β parameter values of the Beta distribution $B(t')$, to which we would like to map the photon nanotime data. A parameter continuous scale should be decided. I think the scale should be mean lifetime going from 0 ns and all the way to the intrinsic dye lifetime, in the absence of acceptor, τ_D. This should then be compared with the scale of mean values in the Beta distribution, from 1 to 0, respectively:

$$\langle \tau \rangle \in \{0, \tau_D\} \Rightarrow \langle t' \rangle \in \{1, 0\} \tag{S18}$$

Then we can use Eq. S17 to start mapping photon nanotime of a given photon stream to a parameter that will correspond to the framework of mpH^{2}MM.

5 Supplementary Data

Additional mpH^{2}MM analyses of HP3 at different NaCl concentrations, and additional controls of the RP$_o$ complex without RNAP.

5.1 E-S figures

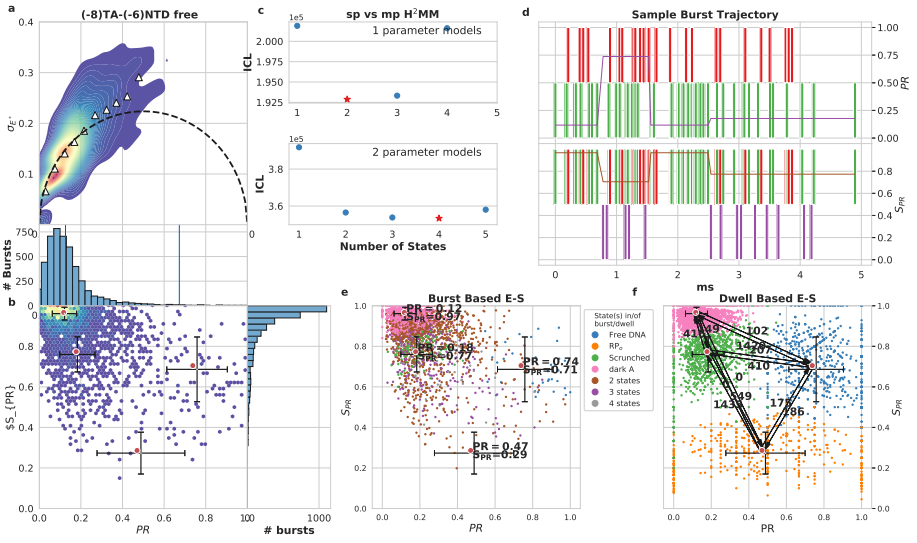

Figure S1: **(-8)TA-(-6)NTD Free promoter** transition rates in e in s^{-1}

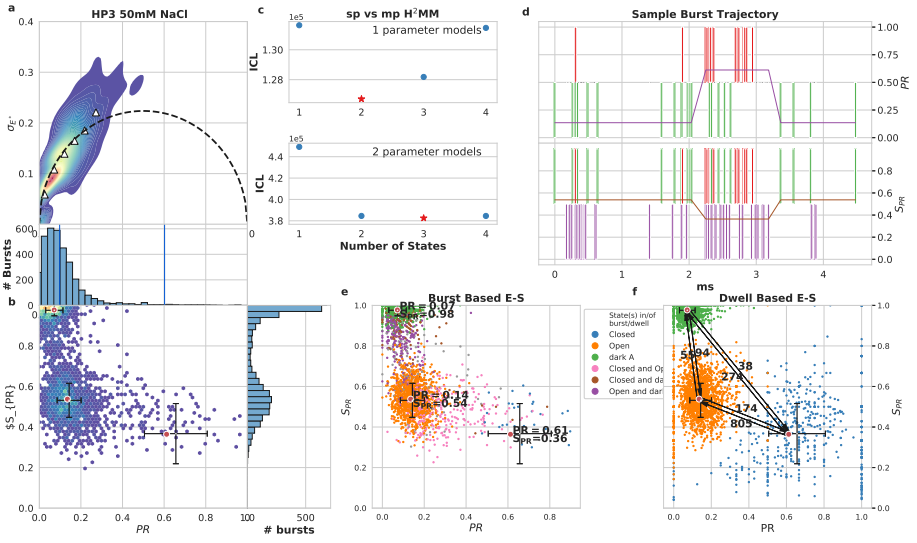

Figure S2: **DNA hairpin, 50 mM NaCl Donor Active Selection** transition rates in e in s^{-1}

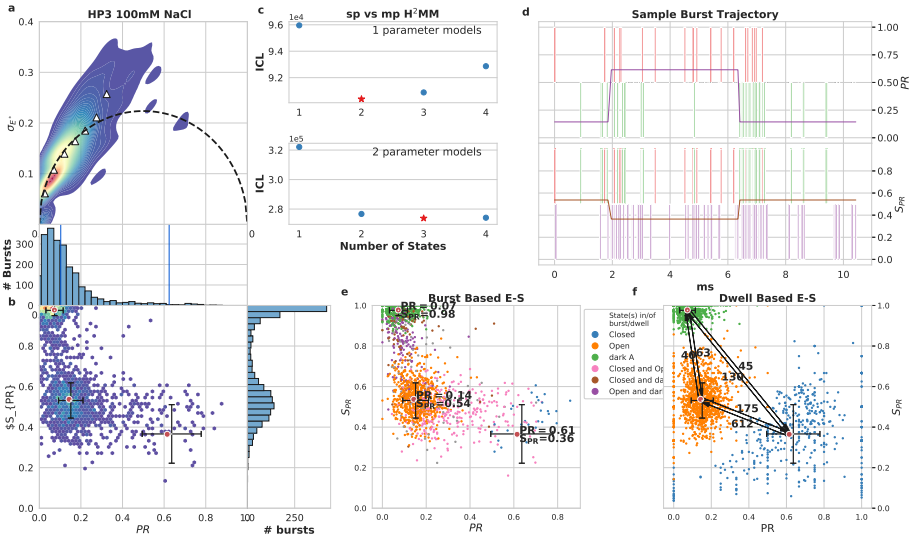

Figure S3: **DNA hairpin, 100 mM NaCl Donor Active Selection** transition rates in e in s^{-1}

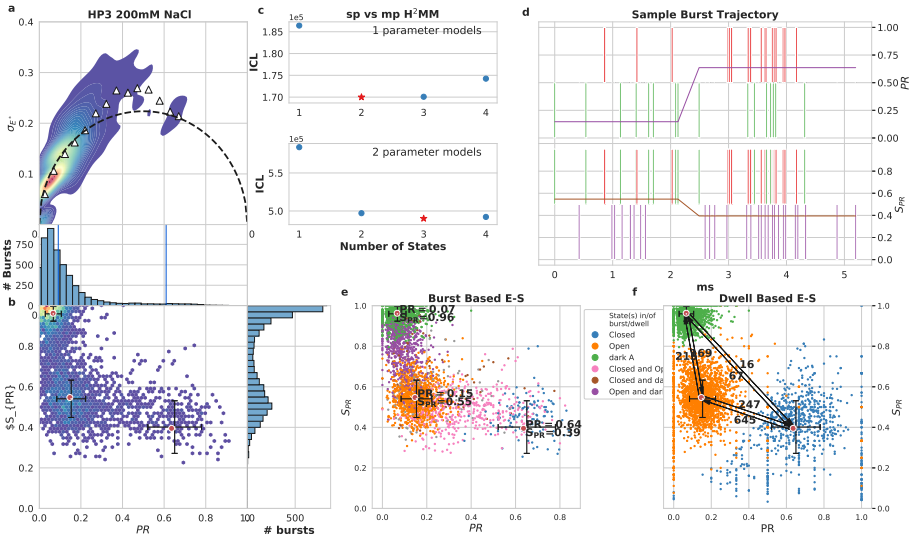

Figure S4: **DNA hairpin, 200 mM NaCl Donor Active Selection** transition rates in e in s^{-1}

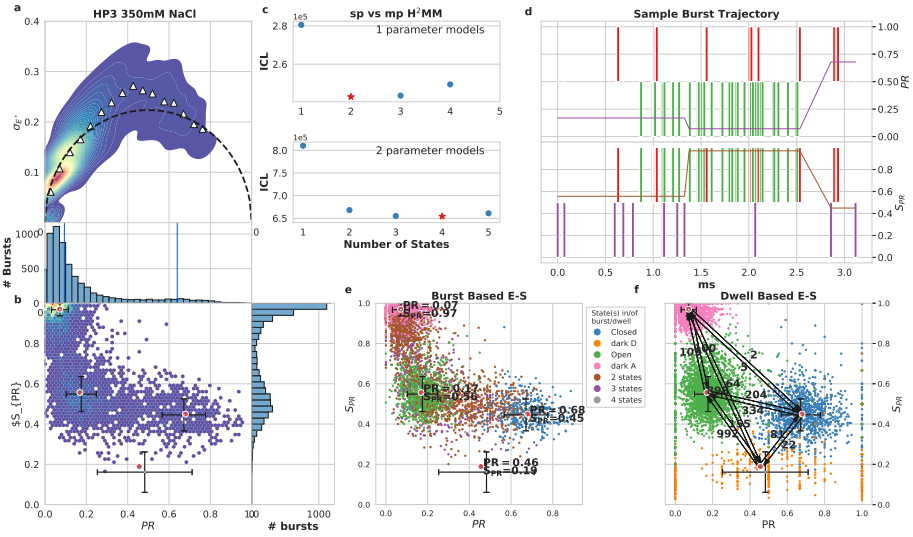

Figure S5: **DNA hairpin, 350 mM NaCl Donor Active Selection**

5.2 Dwell histograms

We now present the analysis of dwell times with comparison to the transition rates derived from the H^2MM model.

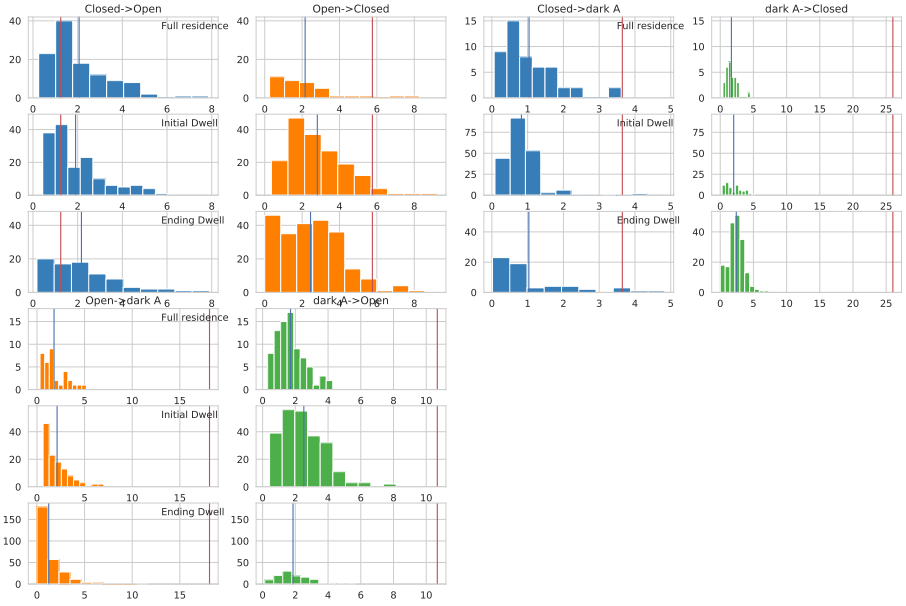

Figure S6: Dwell histograms for DNA hairpin at 50 mM NaCl, Donor Active burst selection

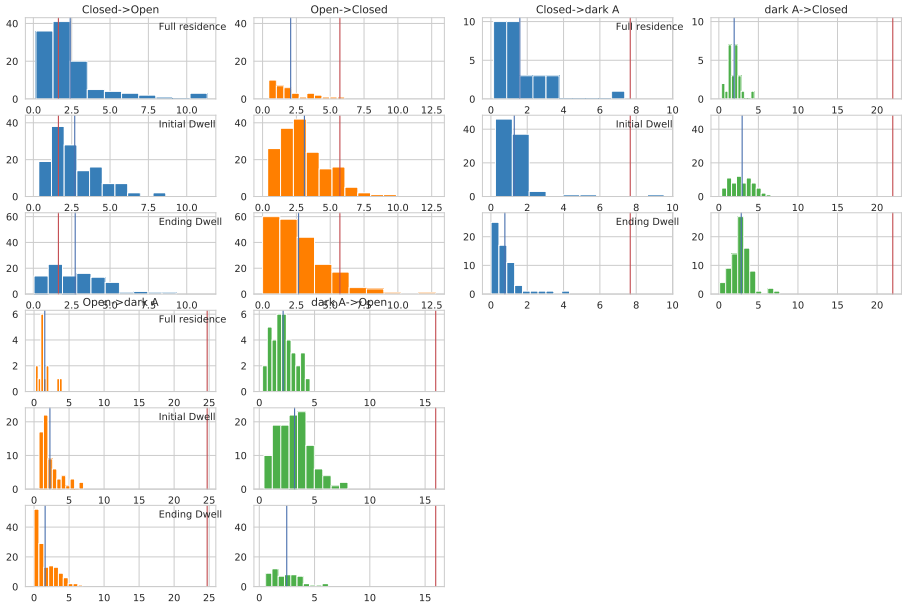

Figure S7: **Dwell histograms for DNA hairpin at 100 mM NaCl, Donor Active burst selection**

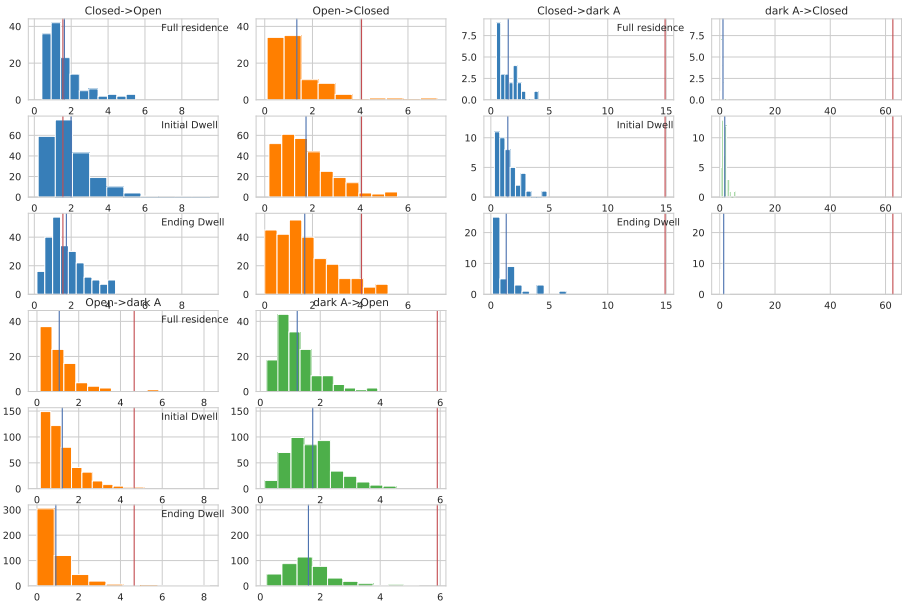

Figure S8: **Dwell histograms for DNA hairpin at 200 mM NaCl, Donor Active burst selection**

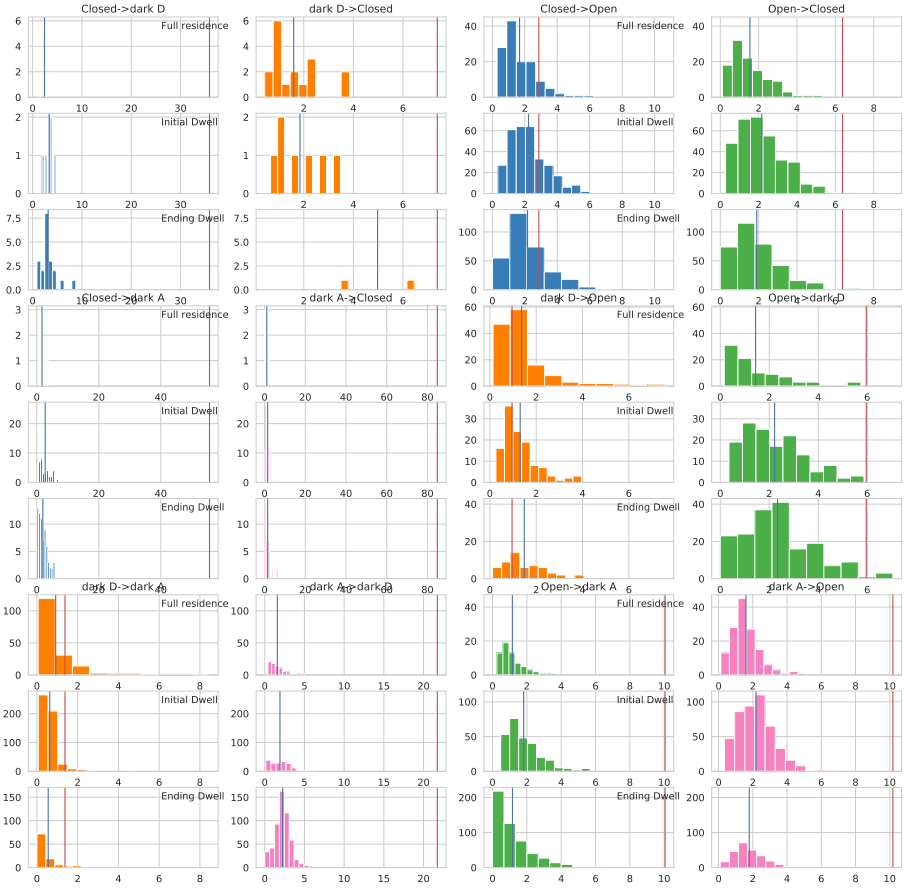

Figure S9: Dwell histograms for DNA hairpin at 300 mM NaCl, Donor Active burst selection

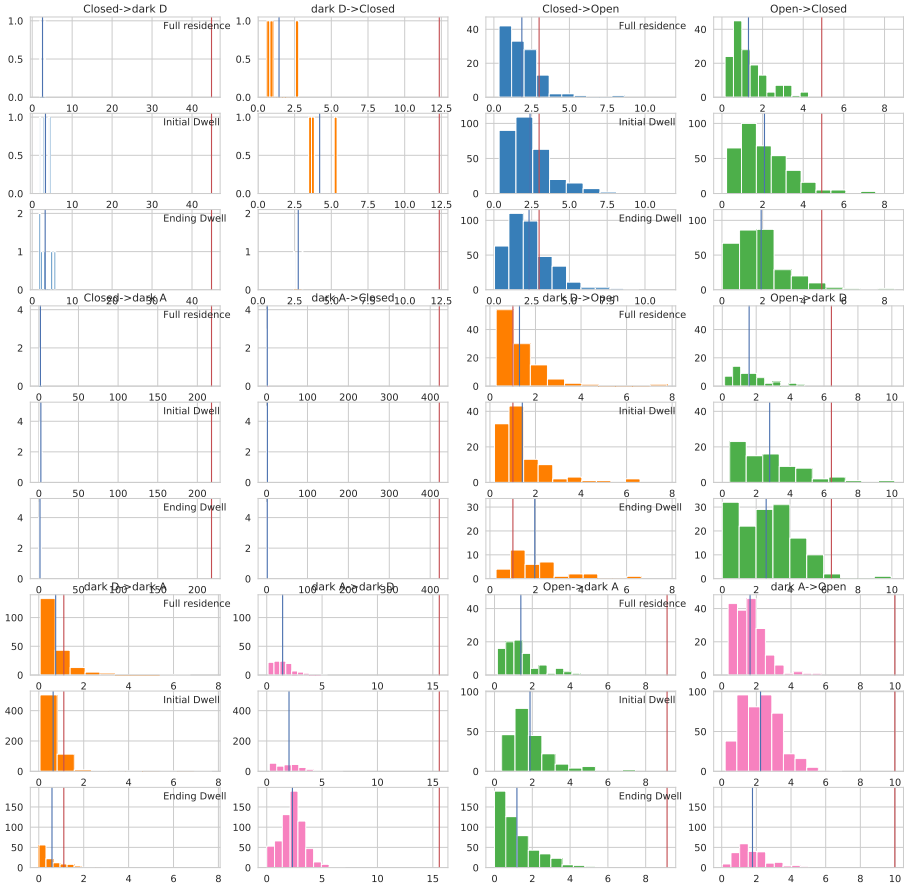

Figure S10: Dwell histograms for DNA hairpin at 350 mM NaCl, Donor Active burst selection

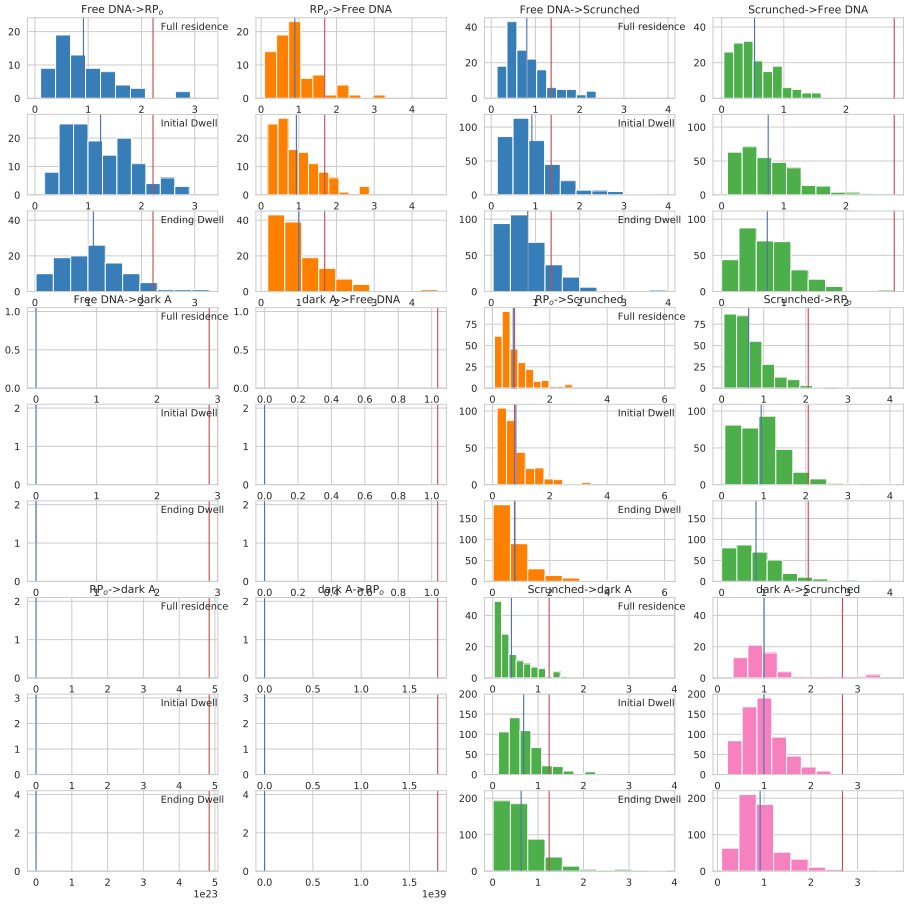

Figure S11: Dwell histograms for (-8)TA(-6)NTD RNAP bound, Donor Active burst selection

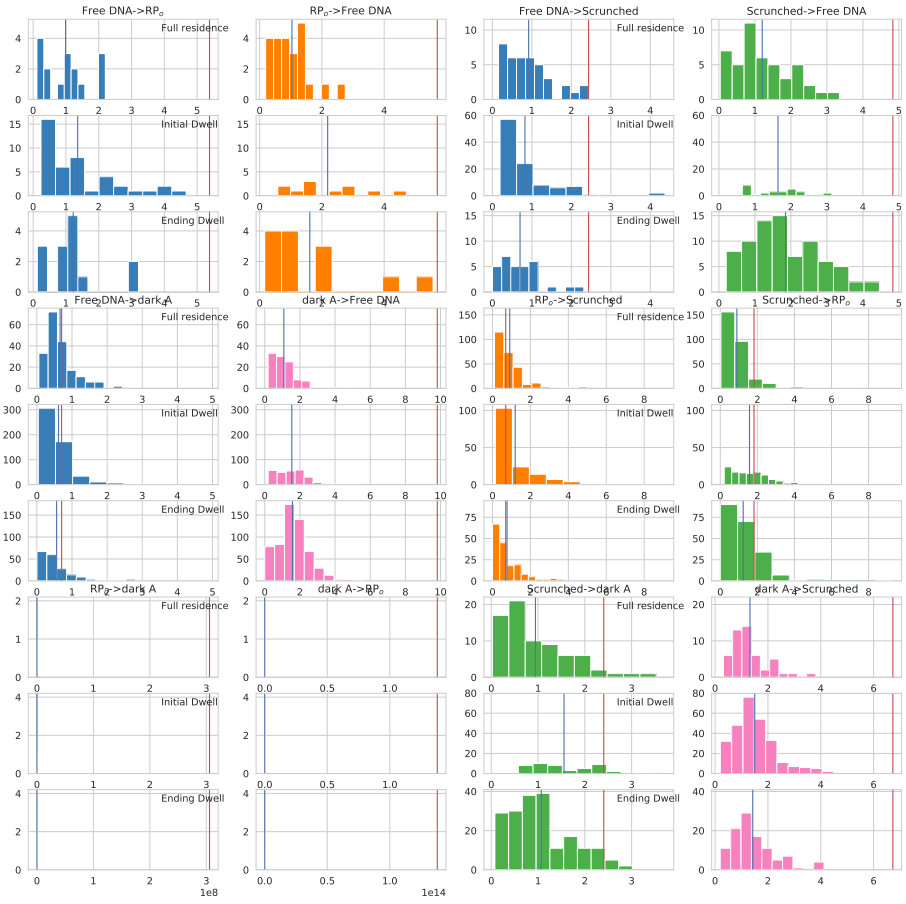

Figure S12: Dwell histograms for (-8)TA-(-6)NTD free promoter, Donor Active burst selection

5.3 Nanotime Histograms

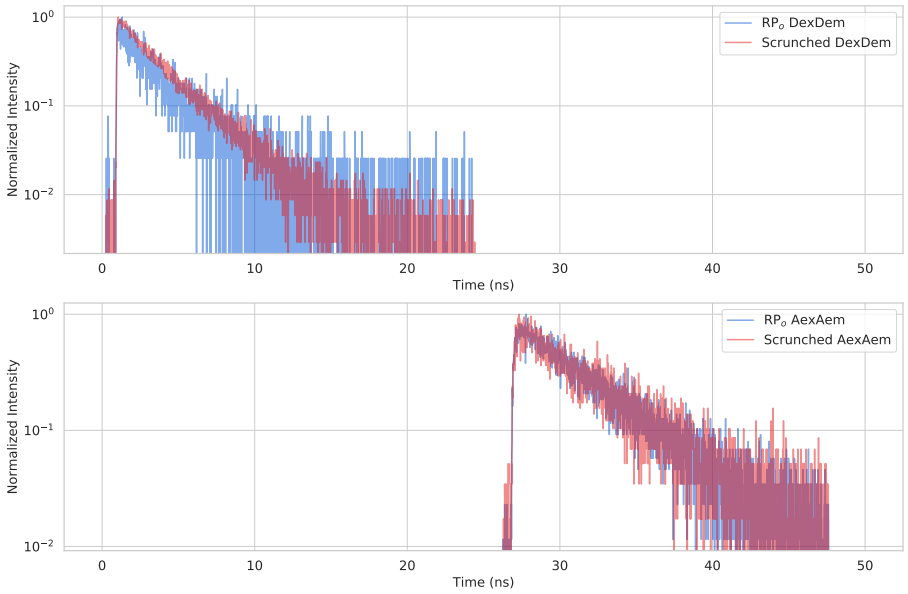

Figure S13: **(-8)TA-(-6)NTD RNAP bound RP$_o$ fluorescent decays.** Histograms of the nanotimes of DexDem (top) and AexAem (bottom) photons assigned to the open and scrunched bubbles sub-populations by *Viterbi* algorithm.

5.4 Tables

Table S1: PR and S_{PR} values for DNA hairpin at 300 mM NaCl

	spH^{2}MM		mpH^{2}MM	
	2-state	3-state	4-state	
ICL[a]	275158.975068564	275353.375540217	756092.749982401	
	PR	PR	PR	S_{PR}
Open[b]	0.09	0.18	0.16	0.56
Closed[c]	0.63	0.68	0.67	0.46
dark A[d]	–	0.07	0.07	0.97
dark D[e]	–	–	0.46	0.17

[a]ICL values are not directly comparable between spH^{2}MM and mpH^{2}MM, as the data set treated by spH^{2}MM probes less photons than by mpH^{2}MM.

[b]The state whose PR, and S_{PR} values best correspond to that predicted for the open conformation, namely a PR≈0.17, and S_{PR}≈0.5

[c]The state whose PR, and S_{PR} values best correspond to that predicted for the open conformation, namely a PR≈0.65, and S_{PR}≈0.5

[d]Dark Acceptor, identified in the three-state spH^{2}MM as the state with the lowest PR, while more easily identified as having a PR≈0 and S_{PR}≈1

[e]Dark Donor, identified as having an S_{PR}≈0, not detectable in spH^{2}MM

Table S2: The transition rate constants for selected H^2MM models of the DNA hairpin at 300 mM NaCl, states are named as in table S1

Open & Closed all values in s^{-1}					
Open to Closed			Closed to Open		
2-state sp[a]	3-state sp[b]	4-state mp[c]	2 state sp	3 state sp	4 state mp
90	217	157	407	409	349
Open & dark A					
Open to dark A			dark A to Open		
2 state sp	3 state sp	4 state mp	2 state sp	3 state sp	4 state mp
–	*20*[d]	99	–	*92*[d]	98
Closed & dark A					
Closed to dark A			dark A to Closed		
2 state sp	3 state sp	4 state mp	2 state sp	3 state sp	4 state mp
–	*57*[d]	18	–	*3*[d]	12
Open & dark D					
Open to dark D			dark D to Open		
2 state sp	3 state sp	4 state mp	2 state sp	3 state sp	4 state mp
–	–	168	–	–	1043
Closed & dark D					
Closed to dark D			dark D to Closed		
2 state sp	3 state sp	4 state mp	2 state sp	3 state sp	4 state mp
–	–	*28*[d]	–	–	135
dark A & dark D					
dark A to dark D			dark D to dark A		
2 state sp	3 state sp	4 state mp	2 state sp	3 state sp	4 state mp
–	–	46	–	–	726

[a] 2-state spH^2MM
[b] 3-state spH^2MM
[c] 4-state mpH^2MM
[d] Too few such dwells in all bursts (less than 10)

Table S3: *PR* and S_{PR} values for (-8)TA-(-6)NTD RNAP bound RP_o, states identified as in [10]

	mpH^2MM	
	PR	S_{PR}
Free DNA	0.75	0.65
RP_o	0.44	0.35
Scrunched RP_o	0.24	0.78
Dark Acceptor	0.12	0.96

Table S4: The transition rate constants for selected H^2MM models of (-8)TA-(-6)NTD RNAP bound RP_o, states are named as in table S3

Transition rates of 4-state mpH_2MM, all rates given in s^{-1}			
Free DNA & RP_o		RP_o & scrunched	
Free DNA to RP_o	RP_o to Free DNA	RP_o to scrunched	scrunched to RP_o
451	593	1300	486
Free DNA & scrunched		scrunched & dark Acceptor	
Free DNA to scrunched	scrunched to Free DNA	scrunched to dark A	dark A to scrunched
738	360	804	374
Free DNA and dark A		RP_o and dark A	
Free DNA to dark A	dark A to Free DNA	RP_o to dark A	dark A to RP_o
0^a	0^a	0^a	0^a

[a] Too few dwells to in all such bursts (less than 10)

References

[1] Paul David Harris, Shimon Weiss, and Eitan Lerner. *Multi-parameter photon-byphoton hidden Markov modeling dataset*. Apr. 2021. DOI: 10.5281/ZENODO.4671393. URL: https://zenodo.org/record/4671393.

[2] Antonino Ingargiola et al. "FRETBursts: An open source toolkit for analysis of freely-diffusing Single-molecule FRET". In: *PLoS ONE* 11.8 (2016), pp. 1–27. ISSN: 19326203. DOI: 10.1371/journal.pone.0160716.

[3] Paul David Harris. *H2MMpythonlib: H2MM_C*. Version 2.0.1. Apr. 8, 2021. DOI: 10.5281/zenodo.4671440. URL: https://zenodo.org/record/4671440.

[4] Ted A. Laurence et al. "Probing structural heterogeneities and fluctuations of nucleic acids and denatured proteins". In: *Proceedings of the National Academy of Sciences* 102.48 (Nov. 2005), pp. 17348–17353. DOI: 10.1073/pnas.0508584102. URL: http://www.pnas.org/cgi/doi/10.1073/pnas.0508584102.

[5] Barbara K. Müller et al. "Pulsed interleaved excitation". In: *Biophysical Journal* 89.5 (2005), pp. 3508–3522. ISSN: 00063495. DOI: 10.1529/biophysj.105.064766.

[6] C. Biernacki, G. Celeux, and G. Govaert. "Assessing a mixture model for clustering with the integrated completed likelihood". In: *IEEE Transactions on Pattern Analysis and Machine Intelligence* 22.7 (July 2000), pp. 719–725. ISSN: 01628828. DOI: 10.1109/34.865189. URL: http://journals.sagepub.com/doi/10.1177/003591577406700922%20http://ieeexplore.ieee.org/document/865189/.

[7] Gilles Celeux and Jean-Baptiste Durand. "Selecting hidden Markov model state number with cross-validated likelihood". In: *Computational Statistics* 23.4 (Oct. 2008), pp. 541–564. ISSN: 0943-4062. DOI: 10.1007/s00180-007-0097-1. URL: http://link.springer.com/10.1007/s00180-007-0097-1.

[8] Nam Ki Lee et al. "Accurate FRET measurements within single diffusing biomolecules using alternating-laser excitation". In: *Biophysical Journal* 88.4 (2005), pp. 2939–2953. ISSN: 00063495. DOI: 10.1529/biophysj.104.054114. URL: http://dx.doi.org/10.1529/biophysj.104.054114.

[9] Menahem Pirchi et al. "Photon-by-Photon Hidden Markov Model Analysis for Microsecond Single-Molecule FRET Kinetics". In: *Journal of Physical Chemistry B* 120.51 (2016), pp. 13065–13075. ISSN: 15205207. DOI: 10.1021/acs.jpcb.6b10726.

[10] Eitan Lerner, Antonino Ingargiola, and Shimon Weiss. "Characterizing highly dynamic conformational states: The transcription bubble in RNAP-promoter open complex as an example". In: *The Journal of Chemical Physics* 148.12 (Mar. 2018), p. 123315. ISSN: 0021-9606. DOI: 10.1063/

1.5004606. URL: http://dx.doi.org/10.1063/1.5004606%20http://aip.scitation.org/doi/10.1063/1.5004606.